ELSEVIER

Journal of Luminescence 81 (1999) 189–197

JOURNAL OF LUMINESCENCE

# Strong coherent interaction of $Nd^{3+}$–$Nd^{3+}$ pair ions in $CaF_2$ crystal[1]

T.T. Basiev, V.V. Fedorov, A.Ya. Karasik, K.K. Pukhov*

*Scientific Center for Laser Materials and Technologies of General Physics Institute, Bild 'D', 38 Vavilov street, 117942, GSP-I, Moscow, Russia*

Received 10 October 1997; received in revised form 14 July 1998; accepted 13 October 1998

**Abstract**

Excited Kramers fine level splittings of $Nd^{3+}$ pair (M) and quartet (N) clusters in $CaF_2$ crystal have been found and investigated by using absorption spectroscopy and accumulated photon echo (APE) techniques. Absorption spectra on the $^4I_{9/2} \rightarrow {}^4G_{5/2}$ transition between Kramers states split into four lines with overall splitting $\sim 5\ cm^{-1}$ ($T = 9$ K, $NdF_3$ concentration 0.1, 0.3 and 1 wt%). At the picosecond laser excitation of the M- and N-centers on the same transition the APE kinetics was observed to be strongly modulated with multiple coherent beatings on pico- and nano-second time scale. Fast Fourier Transform (FFT) of the APE kinetics decay shows that nearest-neighbour absorption lines splittings 0.9, 1.5 and 2.1 $cm^{-1}$ (M-center) are clearly defined in FFT spectrum. Theoretical study revealed that in general case the electrostatic interionic coupling lifts completely the eightfold degeneracy of the excited level of a pair of similar ions. The selection rules for the forced electric-dipole, magnetic dipole and quadrupole intermultiplet transitions are stated. It is suggested that in the case of $Nd^{3+}$–$Nd^{3+}$ pair in $CaF_2$ (M-center), the strong quadrupole–quadrupole coupling is responsible for the fine splitting of the excited $^4I_{9/2} \times {}^4G_{5/2}$ levels and leads to delocalization of the optical electrons within ion pair. 

*Keywords:* Kramers ions; Pairs; Coherent interaction; Level splitting; Quadrupole–quadrupole coupling

## 1. Introduction

Ion pair in crystalline matrix is a unique complex for a study of ion–ion interaction, energy transfer, delocalization, upconversion and cross-relaxation processes. Small distance between ions in the ion pair allows strong exchange, magnetic dipole–dipole, and electric multipole ion–ion interactions [1], which can lift degeneracy and split levels of the ion pair [1–4]. As a result of ions coupling, the splitting values, due to different types of interactions, can be varied in wide kHz–GHz frequency interval [3]. Different experimental methods were used to study ion–ion coupling in the pair and quartet centers [1–5]. Electron paramagnetic resonance (EPR) was found to be effective to study spin-spin interaction and splitting in the ground $^4I_{9/2}$ state of $Nd^{3+}$ [5]. Absorption and fluorescence spectroscopy based, in particular, on narrow-band laser excitation, is useful for such a study of the excited states [2,3]. Coherent ion–ion interaction takes place during the optical dephasing time, hence the photon echo technique is the perspective

* Corresponding author. Tel.: + 7 93 1328376; fax: + 7 093 1350270; e-mail: pukhov@lss.mail.gpi.ru.

[1] The paper was presented at DPC'97.

0022-2313/99/$ – see front matter 
PII: S0022-2313(98)00169-0

for study of strong coupling in ion pair with very high frequency resolution [6].

Recently, we used the accumulated photon echo (APE) technique to study $Nd^{3+}$–$Nd^{3+}$ ion pairs coherent beating due to spin–spin interactions in deluted $Nd^{3+}:CaF_2$ crystals. For zero magnetic field we observed the ground state triplet–singlet level fine splitting ($\sim 0.2\,cm^{-1}$) due to exchange and magnetic dipole–dipole interactions [7]. Now we present experimental and theoretical study of the $Nd^{3+}$–$Nd^{3+}$ coupling on one of the strongest optical transitions between Kramers states $^4I_{9/2}(1) \rightarrow {}^4G_{5/2}(1)$ and show that eightfold degeneracy of the excited Stark levels of the $^4I_{9/2} \times {}^4G_{5/2}$ manifold is lifted due to the electric quadrupole–quadrupole interaction, that can lead to overall splitting up to $\sim 5\,cm^{-1}$. This strong coherent ion–ion interaction can be responsible for ultrafast picosecond delocalization of the electronic excitation within a pair or quartet cluster centers.

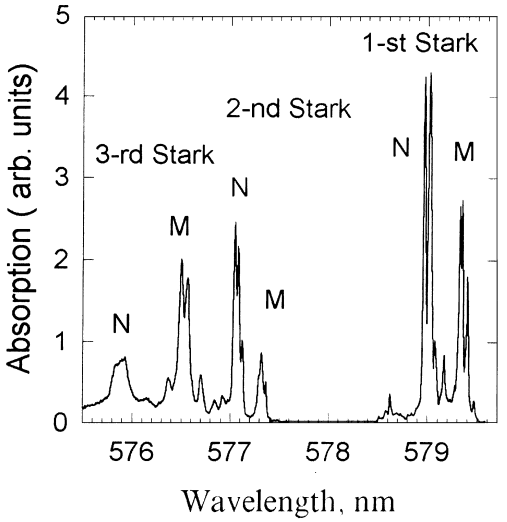


Fig. 1. Low temperature $T = 9$ K absorption spectrum for the $^4I_{9/2} \rightarrow {}^4G_{5/2}$ optical transition of $Nd^{3+}$ ions in $CaF_2$ with $NdF_3$ concentration 0.3 wt%.

## 2. Experimental results

Experimental study of $Nd^{3+}$–$Nd^{3+}$ coupling in the M-center was done both in frequency and time domain with the help of high resolution absorption spectroscopy and APF technique at low 10 K temperature.

We measured a number of absorption spectra on the $^4I_{9/2} \rightarrow {}^4G_{5/2}$ transitions in $CaF_2$-$NdF_3$ with various concentration of $NdF_3$: 0.1, 0.3, and 1.0 wt%. Fig. 1 shows a fragment of the spectrum, that corresponds to the transitions between the lowest Stark level of the $^4I_{9/2} \times {}^4I_{9/2}$ manifold and three lower laying Stark levels of the $^4I_{9/2} \times {}^4G_{5/2}$ manifold for $NdF_3$ concentration of 0.3 wt% ($T = 9$ K). Fig. 2 shows the variation of the absorption spectrum with the $NdF_3$ concentration. For each inter Stark transition, the spectrum consists of the two groups of lines with up to 4 lines for the group. The longer wavelength group for each transition was identified as belonged to the M-type of pair ($Nd^{3+}$–$Nd^{3+}$) optical centers (Fig. 3), and the shorter wavelength one, to the N-type of quartet $(Nd^{3+} - Nd^{3+})_2$ optical centers, that is in a good agreement with data of Refs. [8,9]. The minimum line widths in Figs. 1 and 2 are equal to

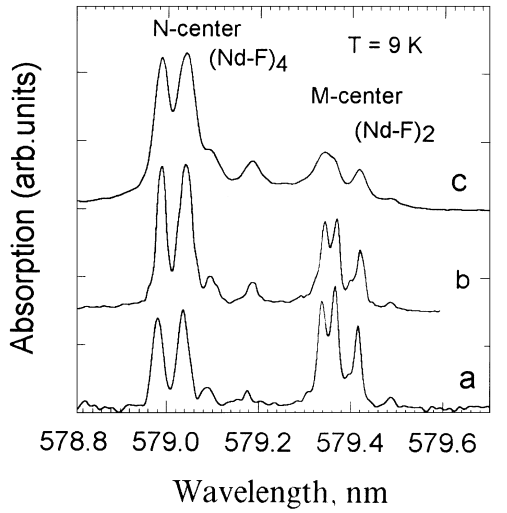


Fig. 2. Absorption spectrum of the fine quartet splitting for the M-pair and N-quartet centers of the $Nd^{3+}$ ions on $^4I_{9/2} \rightarrow {}^4G_{5/2}$ transition in $CaF_2$ with different 0.1 (a), 0.3 (b) and 1.0 (c) wt% $NdF_3$ concentrations at 9 K.

0.02 nm and defined by the spectrometer resolution and (or) by inhomogeneous line broadening.

The M-center consists (Fig. 3) of two $Nd^{3+}$ ions substituting two closest neighboring $Ca^{2+}$ ions

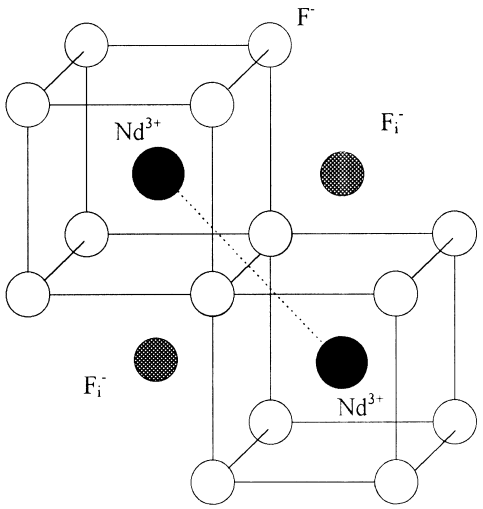


Fig. 3. The structure of $Nd^{3+}$–$Nd^{3+}$ pair center in $CaF_2$ crystal [5,8].

located at $\langle 1\,1\,0\rangle$ crystallographic direction of $CaF_2$ cubic lattice [8] with the distance between $Nd^{3+}$ ions in pair as small as 0.385 nm. The excessive positive charge is compensated by two negative $F^-$ ions in neighboring to $Nd^{3+}$ interstitials. Both of the $Nd^{3+}$ in ion pair are located in the same crystal field. The $Nd^{3+}$ ions environment possesses three orthogonal $C_2$ symmetry axes $x$, $y$, $z$ ($z$-axis passes through the $Nd^{3+}$ ions and $x$-axis passes through the interstitial $F^-$ ions, Fig. 3) [5,8]. More complex N-center $(Nd\text{-}F)_4$ consists of 4 neighbouring Nd ions and is built up from two similar M-centers $(Nd\text{-}F)_2$.

The original result of our study is the observation of quartet type fine splitting $\sim 5\ cm^{-1}$ for both M- and N-centers (see Figs. 1 and 2). This fine splitting and intensity distribution (Fig. 2) do not depend on overall Nd concentration (between 0.1 and 1.0 wt%), although variations in partial absorption and partial concentration of M- and N-centers are very substantial. Previously only doublet splitting was observed between the lowest Stark levels of the $^4I_{9/2}(1) \rightarrow {}^4G_{5/2}(1)$ transition [9].

The investigation of absorption spectrum of transitions $^4I_{9/2} \rightarrow {}^4I_{I3/2}$, $^4I_{I5/2}$, $^4F_{3/2}$ with the help of Fourie spectrometer allowing to get high resolution at temperature T = 4.2 K has shown the absence of splitting exceeding inhomogeneous broadening ($\Delta\nu = 0.8\ cm^{-1}$). This points to the close magnitudes of crystal field potentials and coincidence of the crystal field symmetry for both the $Nd^{3+}$ ions positions in M-pair center and for all the four $Nd^{3+}$ positions in quartet N-center. Besides the time resolved spectroscopy under selective laser absorption saturation confirms that the most of the fine structure lines at the transition $^4I_{9/2} \rightarrow {}^4G_{5/2}$ are caused by the splitting of degenerate levels in strongly coupled $Nd^{3+}$–$Nd^{3+}$ clusters.

To study excitation dynamics and improve spectral resolution we used the APE techniques with picosecond time resolution [7]. Fig. 4a and 4b show APE kinetics for the M-center in $CaF_2$: $Nd^{3+}$ (0.3 wt%) crystal excited by laser pulses with duration $\Delta t = 18$ ps, $\lambda_{exc} = 579.36$ nm, $T = 10$ K. As one can see, we observe strong coherent temporal beatings with multiple time intervals and complicated frequency spectrum, that is due to interference of several coherent, simultaneously excited transitions. Analysis of the APE kinetics (Fig. 4b) with the help of the Fast Fourier transform (FFT) in frequency domain (Fig. 4c) allowed us to reveal two type of fine splittings. The 1st type – small splittings (1.4–6 GHz) reflect subnanosecond beatings with periods 0.71, 0.185 and 0.17 ns. (The experimental resolution was better than 0.04 GHz and determined by used optical delay line.) We can explain this splitting in the frame of the $Nd^{3+}$–$Nd^{3+}$ spin–spin coupling via magnetic dipole–dipole and exchange interactions in the $^4I_{9/2}(1) \times {}^4I_{9/2}(1)$ pair ground manifold. Triplet–singlet level diagram for the $^4I_{9/2}(1) \times {}^4I_{9/2}(1)$ ground manifold of the M-centers was obtained and discussed in Ref. [7].

The 2nd group of picosecond high frequency coherent beatings with the periods of 38, 23 and 16 ps (20–100 GHz) corresponds to quartet (M-center) splittings with $\Delta\nu = 0.9$–$4.5\ cm^{-1}$, observed in the absorption spectrum (Figs. 1 and 2). Arrows in the FFT spectrum (Fig. 4c) correspond to the splitting values from the absorption spectrum (Fig. 2). One can see that the positions of the arrows correspond very well to the peaks in FFT spectrum. The fact, that these fine level splittings are exhibited in temporal beatings of APE decay on time scale much shorter of the optical dephasing time $T_2$, leads us to the assumption that splittings

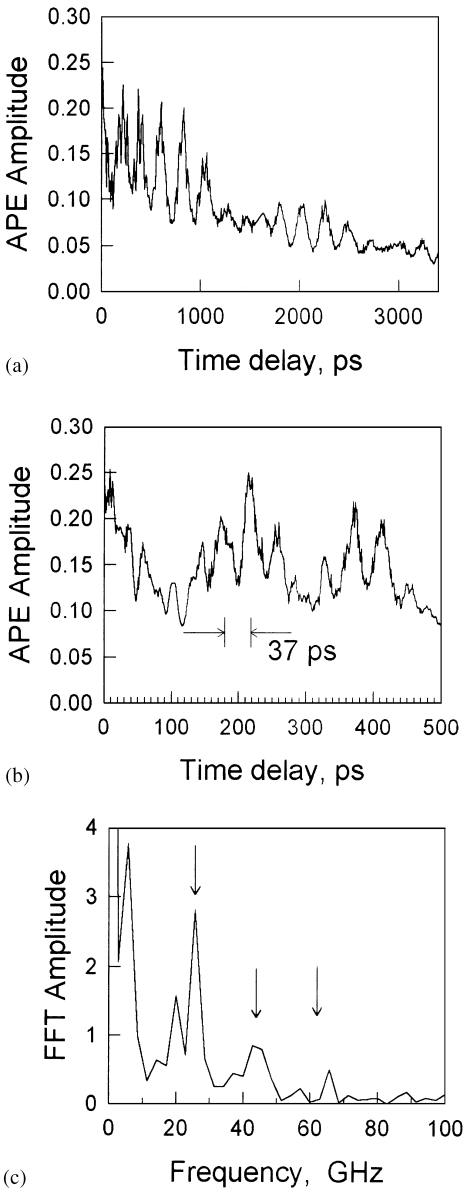


Fig. 4. Accumulated photon echo kinetics (a, b) in $CaF_2 : Nd^{3+}$ ($NdF^3$ concentration 0.3 wt%) crystal under the picosecond laser excitation of the M-center (wavelength of excitation 579.36 nm) and Fast Fourier Transform (c) of the APE signal of Fig. 3b.

in absorption spectrum for M- and N-centers (Fig. 1) arise from coherent $Nd^{3+}$–$Nd^{3+}$ pair interactions. Below we will try to theoretically analyze and estimate these fine level splittings for the excited $^4I_{9/2} \times {}^4G_{5/2}$ manifold due to strong coherent $Nd^{3+}$–$Nd^{3+}$ coupling in the pair of neighboring $Nd^{3+}$ ions (M-centers).

## 3. Theory

### 3.1. Structure of energy sublevels of Kramers ion pair coupled by Coulomb interaction

Energy levels of Kramers ions are at least twofold degenerate in absence of a magnetic field. Let us denote states of Kramers doublet as $\xi$ and $\bar{\xi}$. These states possess by next properties

$$\hat{\theta}\xi = \bar{\xi}, \quad \hat{\theta}\bar{\xi} = -\xi, \tag{1}$$

where $\hat{\theta}$ is the time-reversal operator [1]. Excited energy level of a pair noninteracting $a$ and $b$ ions have eightfold degeneracy [4] with states

$$\varphi_1 = \xi_{1a}\xi_{2b},\ \varphi_2 = \xi_{2a}\xi_{1b},\ \varphi_3 = \bar{\xi}_{1a}\bar{\xi}_{2b},\ \varphi_4 = \bar{\xi}_{2a}\bar{\xi}_{1b}, \tag{2}$$

$$\varphi_5 = \bar{\xi}_{1a}\xi_{2b},\ \varphi_6 = \xi_{2a}\bar{\xi}_{1b},\ \varphi_7 = \xi_{1a}\bar{\xi}_{2b},\ \varphi_8 = \bar{\xi}_{2a}\xi_{1b}. \tag{3}$$

Here subscripts $1a$ ($1b$) and $2a$ ($2b$) designate ground and excited states of ion $a$ ($b$), respectively. In states $\varphi_1, \varphi_3, \varphi_5, \varphi_7$ ($\varphi_2, \varphi_4, \varphi_6, \varphi_8$) the ion $b$ ($a$) is excited and ion $a$ ($b$) nonexcited. In the case under consideration the ground level is the lowest Stark level of $^4I_{9/2}$ manifold and excited level is the lowest Stark level of the $^4G_{5/2}$ manifold of $Nd^{3+}$ ion.

Here we examine the splitting of eightfold degenerate level of similar Kramers ions under Coulomb interionic interaction

$$V = \sum_{i_a, j_b} e^2/|\boldsymbol{r}_{i_a} - \boldsymbol{r}_{j_b}| = \sum_{\alpha\beta} G_{\alpha\beta} V_\alpha^{(a)} V_\beta^{(b)}, \tag{4}$$

where $\boldsymbol{r}_{i_a}(\boldsymbol{r}_{j_b})$ is radius vector of 4f-electron of ion $a$ ($b$). The right-hand side of Eq. (4) is an expansion of Coulomb interaction $V$ into multipoles. Operators $V_\alpha^{(a)}$ ($V_\beta^{(b)}$) depend on electron coordinates of the ion $a$ ($b$). Operators $V_\alpha^{(a)}$ ($V_\beta^{(b)}$) are time-even. This means that they have property [1].

$$\hat{\theta}\, V_\alpha \hat{\theta}^{-1} = V_\alpha^+, \tag{5}$$

where the operator $V_\alpha^+$ is Hermitian-conjugate with $V_\alpha$.

From Eqs. (1) and (5) the properties of matrix elements are as follows [1]:

$$(\xi_2|V_\alpha|\bar{\xi}_2) = (\xi_1|V_\alpha|\bar{\xi}_1) = 0,$$
$$(\bar{\xi}_1|V_\alpha|\xi_2) = -(\bar{\xi}_2|V_\alpha|\xi_1),$$
$$(\bar{\xi}_1|V_\alpha|\bar{\xi}_2) = (\xi_2|V_\alpha|\xi_1). \quad (6)$$

Let us introduce states

$$\psi_1 = (\varphi_1 + \varphi_2 + \varphi_3 + \varphi_4)/2,$$
$$\psi_5 = (\varphi_1 - \varphi_2 + \varphi_3 - \varphi_4)/2, \quad (7a)$$
$$\psi_2 = (\varphi_5 + \varphi_6 - \varphi_7 - \varphi_8)/2,$$
$$\psi_6 = (\varphi_5 - \varphi_6 - \varphi_7 + \varphi_8)/2, \quad (7b)$$
$$\psi_3 = (\varphi_5 + \varphi_6 + \varphi_7 + \varphi_8)/2,$$
$$\psi_7 = (\varphi_5 - \varphi_6 + \varphi_7 - \varphi_8)/2, \quad (7c)$$
$$\psi_4 = (\varphi_1 + \varphi_2 - \varphi_3 - \varphi_4)/2,$$
$$\psi_8 = (\varphi_1 - \varphi_2 - \varphi_3 + \varphi_4)/2, \quad (7d)$$

Wave functions $\psi_1, \psi_2, \psi_3$ and $\psi_4$ ($\psi_5, \psi_6, \psi_7$ and $\psi_8$) are symmetric (antisymmetric) with respect to the ion interchange a⇔b. We must note that the interaction $V$ is symmetric with respect to the ion interchange a⇔b. As a consequence, matrix elements.

$$V_{ij} \equiv (\psi_i|V|\psi_j) = 0, \quad (j = 1, 2, 3, 4;\ j = 5, 6, 7, 8). \quad (8)$$

Taking into account the Eqs. (6)–(8), we obtain that in the representation $\psi_i$ the operator $V$ is given by the following matrix:

$$\{h_{ij}\} = E_0 + \begin{pmatrix} \hat{F} & 0 \\ 0 & -\hat{F} \end{pmatrix}, \quad (9)$$

where $E_0 = (\xi_{1a}\xi_{2b}|V|\xi_{1a}\xi_{2b})$ and $F$ is a $4\times4$ matrix. Matrix elements $F_{ij} = (\psi_i|V|\psi_j)$ can be expressed in terms of matrix elements $V_{kl} \equiv (\varphi_k|V|\varphi_l)$ as

$$F_{11} = V_{12} + (V_{14} + V_{41})/2,$$
$$F_{12} = -(V_{18} + V_{81})/2 + (V_{16} + V_{61})/2, \quad (10a)$$
$$F_{13} = (V_{18} - V_{81})/2 + (V_{16} - V_{61})/2,$$
$$F_{14} = -(V_{14} - V_{41})/2, \quad (10b)$$
$$F_{22} = V_{56} - (V_{58} + V_{85})/2,$$
$$F_{23} = (V_{58} - V_{85})/2, \quad (10c)$$
$$F_{24} = (V_{18} - V_{81})/2 - (V_{16} - V_{61})/2,$$
$$F_{33} = V_{56} + (V_{58} + V_{85})/2, \quad (10d)$$
$$F_{34} = (V_{18} + V_{81})/2 + (V_{16} + V_{61})/2,$$
$$F_{44} = V_{12} - (V_{14} + V_{41})/2. \quad (10e)$$

As it follows from Eq. (9), electrostatic coupling $V$ splits the 8-fold degenerate level in the general case into 8 sublevels with energies $E_0 \pm E_i$ ($i = 1, 2, 3, 4$) where $E_i$ are eigenvalues of matrix $\hat{F}$ and $E_0$ is the common shift of sublevels. In other words, for every sublevel with the energy $E_0 + E_i$ there is a sublevel with energy $E_0 - E_i$. Notice that when the coupling $V$ is an exchange or magnetic interaction, the operators $V^{(a)}$ and $V^{(b)}$ are time-odd operators. As a result, the level splitting structure will be different from that caused by the electrostatic coupling [4].

### 3.2. Estimation of the splittings

In case of the dipole–dipole electrostatic interactions ($V^{(\mathrm{dd})}$) the value of the splitting ($\Delta_{\mathrm{dd}}$) will be on the order of $d_a d_b / R^3$, where $d_a = |\langle\xi_{1a}|\mathbf{d}_a|\xi_{2a}\rangle|$ and $\mathbf{d}_a = e\sum_{i_a} \boldsymbol{r}_{i_a}$ is an operator of the dipole momentum for 4f-electrons, $R$ is the ion–ion distance (for the $M$-centers in $CaF_2$ R = 0.385 nm). For similar ions $d_a = d_b$. The value $d_a^2$ can be estimated as $e^2 S(J, J')/(2J+1)(2J'+1)$, where $S(J, J')$ is a line strength of the forced electric-dipole transition from the ground manifold $J$ to the excited manifold $J'$ partially allowed by the odd part of the crystal field. This leads to

$$\Delta_{\mathrm{dd}} \sim e^2 S(J, J')[(2J+1)(2J'+1)]^{-1}/R^3. \quad (11)$$

For the $Nd^{3+}$ transitions from the $^4I_{9/2}$ ground state to other multiplets the value $S/(2J+1)(2J'+1)$ for crystals is estimated to be of the order

$10^{-20}$ cm$^2$ or less [10]. Therefore, we obtain $\Delta_{dd} \sim 0.1$ cm$^{-1}$ for the excited level splitting due to the dipole–dipole coupling in the $Nd^{3+}$–$Nd^{3+}$ pair in $CaF_2$. Notice that, when the $V^{(dd)}$ interaction gives a dominant contribution to the overall splitting, the splitting value must correlate with the line strength $S(J, J')$. However, this assumption is not confirmed in our case.

For the quadrupole–quadrupole interaction

$$\Delta_{qq} \sim \frac{e^2\langle r^2\rangle^2}{R^5} |(J\|U^{(2)}\|J')|^2, \tag{12}$$

where $\langle r^2\rangle$ is the mean value of the square of the 4f-electron radius averaged over the 4f-wavefunction, $(J\|U^{(2)}\|J')$ is the second-rank reduced matrix element for the transition from the ground manifold $^{2S+1}L_J$ to the excited manifold $^{2S'+1}L'_{J'}$. Substituting $\langle r^2\rangle = 1.001$ a.u. [11] and $|(^4I_{9/2}\|U^{(2)}\|^4G_{5/2})|^2 = 0.8779$ [12] in Eq. (12) leads to very high quadrupole–quadrupole splitting value $\Delta_{qq} \sim 10$ cm$^{-1}$ for the $Nd^{3+}$–$Nd^{3+}$ pair.

Information on the interactions between the $Nd^{3+}$ ions in the ground $^4I_{9/2} \times {}^4I_{9/2}$ manifold has come from EPR measurements on the isolated $Nd^{3+}$–$Nd^{3+}$ pairs in $CaF_2$ [5], $LaCl_3$ [13–16], $LaBr_3$[13,16], and ethyl sulphates (LaES) [16,17] (the smallest $Nd^{3+}$–$Nd^{3+}$ distances (R) are 0.385, 0.437, 0.451, and 0.711 nm in $CaF_2$, $LaCl_3$, $LaBr_3$, and LaES, respectively [5,16]). Bakers [16] analysis of the $Nd^{3+}$–$Nd^{3+}$ pairs in $LaCl_3$, $LaBr_3$, and LaES has shown that the magnetic dipole–dipole (MDD) and exchange interactions are the main ion–ion interactions. They lead to the overall level splittings of ca 0.3 and 0.4 cm$^{-1}$ for $LaCl_3$ and $LaBr_3$, respectively. The MDD contribution is about 0.1 cm$^{-1}$ for both $LaCl_3$ and $LaBr_3$. In LaEs, the MDD interaction is stronger than other spin–spin (including exchange) interactions by an order of magnitude because the $R$ value is relatively large. For the M-centers in $CaF_2$, both MDD and nondipolar interactions are of the same order and cause the overall splitting on the order of 0.1 cm$^{-1}$ [5,7].

It should be mentioned that in the first-order perturbation treatment, the electric quadrupole–quadrupole (EQQ) interaction merely shifts but does not split the ground Stark level of the Kramers ion pair, as discussed by Baker [17] for the $Nd^{3+}$–$Nd^{3+}$ pair in LaES. The EQQ splitting is caused only by the second order perturbation which involves the high lying Stark levels of ground manifold, whereas the MDD and exchange interactions contribute even to the first-order splitting. For this reason, the effect of the EQQ interaction weakens in the ground state. However, this effect may be significant for the non-Kramers ion pairs or for the Kramers ion pairs with the accidental near-degeneracy of the ground and excited Stark levels [16].

A basically different situation occurs with the excited-state Kramers ion pair. In this case, even the first-order perturbation in EQQ brings about the splitting, similar to the first-order contribution from the MDD and exchange interactions in the ground state. Thus, in the general case, the effect of EQQ interaction is expected to be more significant in the excited states, than in the ground state.

Note that the experimental 1–5 cm$^{-1}$ level splittings occur namely for $^4I_{9/2} \rightarrow {}^4G_{5/2}$ transitions, where the square of the reduced matrix element $(^4I_{9/2}\|U^{(2)}\|^4G_{5/2})^2$ is one of the highest among the different optical transitions in $Nd^{3+}$ ion and is equal to 0.8779, whereas the values of $(^4I_{9/2}\|U^{(2)}\|^{2S+1}L_J)^2$ are less than 0.1 for all other $Nd^{3+}$ transitions [12].

For the excited $^4I_{9/2} \times {}^4G_{5/2}$ manifold of the M-center we found that MDD-induced splitting is no greater than 0.05 cm$^{-1}$ (to calculate the MDD splitting, the next values of the reduced matrix elements were used: $(^4I_{9/2}\|L + 2S\|^4I_{9/2}) = 11.2589$ and $(^4G_{5/2}\|L + 2S\|^4G_{5/2}) = 4.2592$ [18]).

Based on the above arguments we suppose that the EQQ interaction is mainly responsible for the observed level splitting. Our suggestion are confirmed by Ref. [9], where all $Nd^{3+}$ transitions from the ground to high lying multiplets with energy up to 28 000 cm$^{-1}$ were studied with high accuracy using the absorption spectroscopy. For the M- and N-centers 1 cm$^{-1}$ splittings were observed in Ref. [9] only for the transition between lowest Stark level of the $^4I_{9/2}$ ground and 3 Stark levels of the $^4G_{5/2}$ states, whereas no splittings were observed with accuracy $\Delta \ll 1$ cm$^{-1}$ for other inter-Stark transitions in the 0–28 000 cm$^{-1}$ energy range. These results suggest that it is unlikely that the

exchange interactions make essential contribution to the splitting value of the $^4I_{9/2} \times {}^4G_{5/2}$ levels.

### 3.3. Quadrupole–quadrupole splitting

Let us investigate the EQQ interaction in detail. Using the expression [19,20] for the expansion of Coulomb potential in spherical harmonics, the quadrupole–quadrupole interaction ($V^{(qq)}$) between the pair of similar rare-earth ions in $^{2S+1}L_J \times {}^{2S'+1}L'_{J'}$ manifold can be written as

$$V^{(qq)} = C_{qq} \sum_{m=-2}^{2} G_m V_m^{(a)} V_{-m}^{(b)}, \tag{13}$$

were

$$C_{qq} = \frac{e^2 \langle r^2 \rangle}{R^5} |(^{2S+1}L_J \| U^{(2)} \| {}^{2S'+1}L'_{J'})|^2 \tag{14}$$

is the constant of the quadrupole–quadrupole interaction; $G_m = G_{-m} = 7 \times 32/[(2+m)!(2-m)!5]$; matrix elements of operators $V_m$ in the $|J,M\rangle$ representation are directly proportional to the 3j-symbol:

$$\langle JM|V_m|J'M'\rangle = (-1)^{J_{max}-M} \begin{pmatrix} J & 2 & J' \\ -M & m & M' \end{pmatrix}; \tag{15}$$

the $z$-axis for $a$ and $b$ ions are taken to be parallel to the line joining RE ions in pair. In the general case, the states $\xi$ and $\bar{\xi}$ are of the form [1]

$$|\xi\rangle = \sum_M C_{J,M} |J, M\rangle, \tag{16a}$$

$$|\bar{\xi}\rangle = \sum_M C^*_{J,M} (-1)^{J-M} |J, -M\rangle. \tag{16b}$$

The point symmetry at the $Nd^{3+}$ ions consisting of an M-center belongs to $C_{2v}$. In this case, the values of the magnetic quantum number $M$ in Eq. (16a) differ by at least two units because of binary symmetry [1]:

$$|\xi_1\rangle = C_{9/2,9/2}|9/2, 9/2\rangle + C_{9/2,5/2}|9/2, 5/2\rangle + C_{9/2,1/2}|9/2, 1/2\rangle + C_{9/2,-3/2}|9/2, -3/2\rangle + C_{9/2,-7/2}|9/2, -7/2\rangle, \tag{17}$$

$$|\xi_2\rangle = C_{5/2,5/2}|5/2, 5/2\rangle + C_{5/2,1/2}|5/2, 1/2\rangle + C_{5/2,-3/2}|5/2, -3/2\rangle. \tag{18}$$

For this reason $F_{12} = F_{13} = F_{21} = F_{24} = F_{31} = F_{34} = F_{42} = F_{43} = 0$. Besides, all the $C_{J,M}$ in Eq. (16a) can be chosen to be real. This assumption leads to $F_{14} = F_{23} = F_{32} = F_{41} = 0$. As a result, we obtain that states $\psi_i$ are "correct" zero-order eigenstates with eigenvalues $E_0 + \Delta_i$, where

$$\Delta_1 = V_{12}^{(qq)} + V_{14}^{(qq)}, \quad \Delta_2 = V_{56}^{(qq)} - V_{58}^{(qq)}, \tag{19a}$$

$$\Delta_3 = V_{56}^{(qq)} + V_{58}^{(qq)}, \quad \Delta_4 = V_{12}^{(qq)} - V_{14}^{(qq)} \tag{19b}$$

$$\Delta_5 = -\Delta_1, \quad \Delta_6 = -\Delta_2,$$

$$\Delta_7 = -\Delta_3, \quad \Delta_8 = -\Delta_4. \tag{19c}$$

The EQQ constant $C_{qq}$ in Eq. (14) is equal to 9.68 $cm^{-1}$ for $Nd^{3+}$–$Nd^{3+}$ pair M-centers in $^4I_{9/2} \times {}^4G_{5/2}$ manifold. We calculated the values of overall splitting ($\Delta_{qq}$) for a variety of wave functions $\xi_1$ and $\xi_2$. The calculated values $\Delta_{qq}$ lie between zero (e.g. for $|\xi_1\rangle = |9/2, 9/2\rangle$ and $|\xi_2\rangle = |5/2, 5/2\rangle$) and 14, 92 $cm^{-1}$ (for $|\xi_1\rangle = |9/2, 1/2\rangle$ and $|\xi_2\rangle = |5/2, 1/2\rangle$). To be specific, we need to know coefficients $C_{9/2,M}$ and $C_{5/2,M}$ in Eqs. (17) and (18). Some restrictions on the coefficient $C_{9/2,M}$ impose the experimental values of $g$-factor ($g_{xx} = 2.05$, $g_{yy} = 3.35$, $g_{zz} = 2.05$ [5]). Within this restriction, a wide array of coefficients $C_{9/2,M}$ and $C_{5/2,M}$ was looked over for the calculation of $\Delta_{qq}$. After this treatment the corresponding values $\Delta_{qq}$ for the examined cases were found to be varied in the smaller region 1–7 $cm^{-1}$.

### 3.4. Line intensities

The lowest Stark level in $^4I_{9/2} \times {}^4I_{9/2}$ manifold of the uncoupled Kramers ion pair has fourfold degeneracy. In the coupled pair this level will be split into triplet and singlet states [5,7]. Together with lifting of the eightfold level $^4I_{9/2} \times {}^4G_{5/2}$ degeneracy, the coupling can split a transition from the lowest Stark level of the ground manifold to anyone Stark level of the excited manifold into $4 \times 8$ transitions.

Triplet states ($\chi(T_+)$, $\chi(T_-)$ and $\chi(T_0)$) are symmetric and the singlet ($\chi(S)$) is antisymmetric with respect to the ion interchange a⇔b. The forced

Table 1
Relative intensities of the forced electric-dipole transitions from ground state sublevels $^4I_{9/2}(1) \times {}^4I_{9/2}(1)$ to excited state sublevels $^4I_{9/2} \times {}^4G_{5/2}$

| Transition | Relative intensities | $I_i$ | Remarks |
|---|---|---|---|
| $\chi(S) \to \psi_1$ | $2J_x$ | $2J_x$ | $J_x = \lvert\langle\xi_1\lvert x\rvert\bar{\xi}_2\rangle\rvert^2/A$, |
| $\chi(S) \to \psi_2$ | $2J_z$ | $2J_z$ | $J_y = \lvert\langle\xi_1\lvert y\rvert\bar{\xi}_2\rangle\rvert^2/A$, |
| $\chi(S) \to \psi_3$ | 0 | 0 | $J_z = \lvert\langle\xi_1\lvert z\rvert\bar{\xi}_2\rangle\rvert^2/A$, |
| $\chi(S) \to \psi_4$ | $2J_y$ | $2J_y$ | $A = 8[\lvert\langle\xi_1\lvert x\rvert\xi_2\rangle\rvert^2 + \lvert\langle\xi_1\lvert y\rvert\bar{\xi}_2\rangle\rvert^2\rvert + \langle\xi_1\lvert z\rvert\xi_2\rangle\rvert^2]$, |
| $\chi(T_\pm) \to \psi_5$ | $J_z$ | $1/4 - 2J_x$ | $I_i$ are the averaged relative intensities from $\chi(T_\pm)$, $\chi(T_0)$ and $\chi(S)$ states to $\psi_i$ state |
| $\chi(T_0) \to \psi_5$ | $2J_y$ | | |
| $\chi(T_\pm) \to \psi_6$ | $J_x + J_y$ | $1/4 - 2J_z$ | |
| $\chi(T_0) \to \psi_6$ | 0 | | |
| $\chi(T_\pm) \to \psi_7$ | $J_x + J_y$ | 1/4 | |
| $\chi(T_0) \to \psi_7$ | $2J_z$ | | |
| $\chi(T_\pm) \to \psi_8$ | $J_z$ | $1/4 - 2J_y$ | |
| $\chi(T_0) \to \psi_8$ | $2J_x$ | | |

electric-dipole transitions from the symmetric triplet states to the symmetric states $\psi_1$, $\psi_2$, $\psi_3$ and $\psi_4$ are forbidden. Similarly, the transitions from the antisymmetric state $\chi(S)$ to the antisymmetric states $\psi_5$, $\psi_6$, $\psi_7$ and $\psi_8$ are forbidden too. (These selection rules are similar to those discussed in Ref. [3] for a coupled non-Kramers ion pair $Pr^{3+}$–$Pr^{3+}$ in $LaF_3$.) The relative intensities of the transitions not forbidden by the above-mentioned selection rule are given in Table 1. Let us note that selection rules for magnetic dipole and electric quadrupole transitions are directly opposite: symmetric–symmetric and antisymmetric–antisymmetric transitions are allowed and symmetric–antisymmetric ones are forbidden.

## 4. Discussion

As one can see from Refs. [5,7], the singlet–triplet and triplet–triplet splittings due to spin–spin coupling in the ground state $^4I_{9/2}(1) \times {}^4I_{9/2}(1)$ are much smaller than quadrupole–quadrupole splittings for the excited states $^4I_{9/2} \times {}^4G_{5/2}$ levels and even smaller than the inhomogeneous broadening and spectral resolution in Fig. 4. Therefore we can compare the observed absorption line intensities with the relative intensities $I_i$ ($i = 1, 2, \ldots, 8$), which are the sum of the relative intensities of the transitions from all the triplet–singlet sublevels of the lowest Stark level of the ground $^4I_{9/2}(1) \times {}^4I_{9/2}$ manifold to the exited $\psi_i$ state of $^4I_{9/2} \times {}^4G_{5/2}$ manifold (see Table 1). In the common case, as we can see from Table 1, the theory predicts seven absorption lines with $I_i \leq 1/8$. However, the actual number of lines can be smaller. That has at least two explanations.

- the energies of some sublevels can coincide within the line widths.
- the intensities for different polarizations ($x$, $y$, $z$) can differ strongly from each other.

## 5. Conclusion

We presented new results on the experimental and theoretical investigations of the $Nd^{3+}$–$Nd^{3+}$ pair ions with strong coherent interactions in $CaF_2$ single crystals with $NdF_3$ concentrations of 0.1, 0.3, and 1.0 wt.%. For the M (dimer) and the N (quartet) rhombic centers, at 9 K, the absorption spectra of the optical transition $^4I_{9/2} \to {}^4G_{5/2}$ between the lowest Stark levels were found to consist of two quartet groups of lines. For the M-center the splitting values vary from 0.9 to 4.5 $cm^{-1}$ due to the dynamic $Nd^{3+}$–$Nd^{3+}$ interaction on the optical transition. For the N-centers, these variations were from 1.5 to 6 $cm^{-1}$. At the picosecond excitation of M(N)-centers APE kinetics was observed to be strongly modulated with the multiple coherent beating on the pico- and nano-second time scale. Fast Fourier Transform analysis of the APE kinetics decay shows that the absorption line splitting values 0.9, 1.5, and 2.2 $cm^{-1}$ are well exhibited in the FFT spectrum.

The theory for the excited level splitting due to the strong dynamic coupling of the Kramers ions in the pair was developed. It was revealed that the electrostatic dynamic coupling can lift a degeneracy of the excited level of the uncoupled pair of ions and leads to the fine level splitting on up to 8 sublevels (for non-Kramers ions, the dynamic coupling

splits the excited level only into two sublevels). It was shown that the quadrupole–quadrupole strong coherent interaction gives the main contribution to the dynamic splitting of the $^4I_{9/2} \times {}^4G_{5/2}$ excited levels for $Nd^{3+}$–$Nd^{3+}$ pair. The calculated value of the overall splitting corresponds well with the experimental data.

Due to all these facts and calculations we conclude that the fine level splittings in the absorption spectra and the multiple coherent beatings in APE signal are caused by the strong coherent ion–ion interaction for the pair M- and quartet N-centers. The observation of such a strong coherent, dynamic Nd–Nd coupling demonstrates ultrafst picosecond $\tau^{-1} \sim \Delta_{qq}$ delocalisation of the optical excitation within the neodymium ion pair and quartet clusters that spread over the $CaF_2$ crystal.

## Acknowledgements

The authors are grateful to Prof. M.N. Popova of Institute Spectroscopy for Fourie spectrometer measurements of $^4I_{9/2} \rightarrow {}^4I_{13/2}, {}^4I_{15/2}, {}^4F_{5/2}$ absorption spectra. This work was partially supported by Russian Foundation for Basic Research (project N 97-02-17669), INTAS Contract N 96-0232 and joint RFFI-DFG grant (project N 96-02-00143).

## References

[1] A. Abragam, B. Bleany, Electron Paramagnetic Resonance of Transition Ions, Clarendon Press, Oxford, 1970.
[2] R.L. Cone, R.S. Meltzer, in: Spectroscopy of Solids Containing Rare Earth Ions, Eds. A.A. Kaplanskii, R.M. Macfarline, North-Holland Physics Publishing, New York, 1987, p. 481 and references therin.
[3] J.C. Vial, R. Buisson, J. Physique-Lett. 43 (1982) L339.
[4] R. Buisson, J. Lumin 31&32 (1984) 78.
[5] N.E. Kask, L.S. Kornienko, E.G. Lariontzev, Fiz. Tverd. Tela (USSR) 8 (1966) 2572.
[6] J.B.W. Morsink, D.A. Wiersma, Chem. Phys. Lett. 65 (1979) 105.
[7] V.V. Fedorov, T.T. Basiev, A.Ya. Karasik, K.K. Pukhov, K.W. Ver Steeg, Conf. Handbook, ICL'96, Prague, pp. 12–73.
[8] V.V Osiko, Yu.K. Voron'ko, A.A. Sobol, Crystals, vol. 10, Springer, Berlin, 1984.
[9] T.P.J. Han, C.D. Jones, R.W. Syme, Phys. Rev. B 47 (1993) 14 706.
[10] W.E. Krupke, IEEE J. Quant. Electron. QE-7 (1971) 153.
[11] A.J. Freeman, R.E. Watson, Phys. Rev. 127 (1962) 2058.
[12] W.T. Carnall, P.R. Fields, K. Rajnak, J. Chem. Phys. 49 (1968) 4424.
[13] J.D. Riley, J.M. Baker, R.G. Birgenau, Proc. Roy. Soc. A 230 (1970) 369.
[14] K.L. Brower, H.J. Stapleton, E.O. Brower, Phys. Rev. 146 (1966) 233.
[15] J.M. Baker, J.D. Riley, R.G. Shore, Phys. Rev. 150 (1966) 198.
[16] J.M. Baker, Rep. Prog. Phys. 34 (1971) 109.
[17] J.M. Baker, Phys. Rev. A 136 (1964) 1633.
[18] A.A. Kornienko, Private communication.
[19] B.C. Carlson, G.S. Rushbrooke, Proc. Cambridge Phil. Soc. 46 (1950) 626.
[20] T. Kushida, J. Phys. Soc. Japan 34 (1973) 1318.